



# Synthesis and thermo-physical properties of water-based novel Ag/ZnO hybrid nanofluids

Surendra D. Barewar<sup>1</sup> · Sandesh S. Chougule<sup>1</sup> · J. Jadhav<sup>2</sup> · S. Biswas<sup>2</sup>

Received: 31 August 2018 / Accepted: 25 October 2018 / Published online: 2 November 2018  
© Akadémiai Kiadó, Budapest, Hungary 2018

## Abstract

The comparative study on the thermo-physical properties of water-based ZnO nanofluids and Ag/ZnO hybrid nanofluids is reported in the present study. The outer surface of ZnO nanoparticles was modified with a thin coating of Ag nanoparticles by a wet chemical method for improved stability and heat transfer properties. The ZnO and Ag/ZnO nanofluids were prepared with varying volume concentration ( $\phi = 0.02\text{--}0.1\%$ ). The synthesized nanoparticles and nanofluids were characterized with different characterization methods viz., scanning electron microscopy, X-ray diffraction, dynamic light scattering, thermal conductivity measurement, and viscosity measurement. Results show that thermal conductivity of Ag/ZnO hybrid nanofluids is found to be significantly higher compared to ZnO nanofluids. The maximum thermal conductivity an enhancement for Ag/ZnO nanofluid ( $\phi = 0.1\%$ ) is found to 20% and 28% when it compared with ZnO nanofluid ( $\phi = 0.1\%$ ) and water, respectively.

**Keywords** ZnO nanofluids · Ag/ZnO hybrid nanofluids · Wet chemical method · Thermal conductivity · Viscosity

## List of symbols

$\mu$	Viscosity (Pa s)
$\phi$	Volume concentration (%)
$m$	Mass (kg)
$\rho$	Density ( $\text{kg m}^{-3}$ )
$k$	Thermal conductivity ( $\text{W m}^{-1} \text{K}^{-1}$ )
$D_c$	Diffusion coefficient
$K_B$	Boltzmann constant
$T$	Absolute temperature
$r$	Radius of the particles

n	Nanoparticles
nf	Nanofluid

## Abbreviations

EG	Ethylene glycol
TC	Thermal conductivity
Ag/ZnO	Silver-coated zinc oxide nanoparticles

## Subscript

b Base fluid (deionized water)

✉ Sandesh S. Chougule  
sandesh\_chougule@yahoo.com

Surendra D. Barewar  
surendra.barewar@gmail.com

J. Jadhav  
jeevan.jdhv@gmail.com

S. Biswas  
sommath@lnmiit.ac.in

<sup>1</sup> Department of Mechanical Engineering, The LNM Institute of Information Technology, Jaipur 302031, India

<sup>2</sup> Department of Physics, The LNM Institute of Information Technology, Jaipur 302031, India

## Introduction

Nowadays, miniaturization of the product by utilizing advanced fabrication techniques is a key to innovation and development in various sectors indicating aerospace, automobile, chemical, power, and electronics. In case of a miniaturized system, thermal management plays a vital role in its reliability and life cycle. For thermal management, various heat transfer enhancement devices have been reported in the literature. The nanofluids can be utilized to improve heat transfer performance in various cooling techniques such as microchannels, heat pipes, heat exchangers, and jet impingement cooling [1–4]. In the first the attempt, Choi et al. [5] reported the significant improvement in thermal conductivity by dispersing nano-sized particles in base fluids. The various nanoparticles namely oxides ( $\text{Al}_2\text{O}_3$ , CuO, ZnO,  $\text{TiO}_2$ ,  $\text{SiO}_2$ ) [6–10],

metallic nanoparticles (Ag, Cu) [11, 12] and carbon-based nanoparticles (carbon nanotubes and graphene) [13] were studied by the various researcher for its heat transfer applications. The thermo-physical properties of these nanofluids primarily depend upon the parameters like concentration, temperature, synthesis method, shape, and size of the nanoparticles [14].

Most of the reported work was based on the use of one type of nanoparticles to enhance the thermo-physical properties of the base fluids. The performance of these nanofluids related to thermal conduction is not up to the mark using either a metal oxide or metallic nanoparticles in the base fluid. The major issue with the use of one type of nanoparticle-based nanofluids is their monopoly in physical and chemical properties [15]. The metallic nanoparticles have good thermal properties (metallic Ag, Cu, etc.) but less stable in the base fluids. On contrary, metal oxide nanoparticles are more stable in base fluids ( $\text{Al}_2\text{O}_3$ , CuO, etc.). However, they have very limited thermal conductivity value. In view of this, nowadays, researchers reported various methods of preparation of hybrid nanofluids [16–24]. Hybrid nanofluid contains a combination of two or more type of nanoparticles in base fluid either by mixing or in situ process. It was observed that the addition of higher conductivity nanoparticles (metallic or carbon based) to the metal oxides significantly enhanced the thermal conductivities of nanofluids. Yarmand et al. [16] studied the graphene coated with Ag to form a nanocomposite (hybrid nanoparticles). They used 0.1% mass concentration of nanoparticles to prepare Ag/graphene nanofluids with water as the base fluid. They reported enhancement in thermal conductivity by 22.22% at 40 °C. Similarly, Baby et al. [17] synthesized CuO-coated graphene hybrid nanoparticles by chemical reduction method. These nanoparticles were used to prepare surfactant-free nanofluids with DI water and ethylene glycol. The maximum enhancement of 28% in thermal conductivity at 0.05% volume concentration was reported. The Ag-mixed multi-walled CNTs without surfactant nanofluid was synthesized by Munkhbayer et al. [18]. For improving stability and thermal conductivity, they prepared hybrid nanofluids by one-step method using pulse power evaporation. Results show that the improvement in thermal conductivity of hybrid nanofluid is found to be 14.5% at 40 °C when it compared with the base fluid. Tadjarodi et al. [19] reported modified surface properties of silica nanoparticles by coating it with metallic Ag nanoparticles. It is observed that in base fluids (ethyl glycol) thermal conductivity was increased by 10.95% by the addition of nanoparticles of 2.5% mass concentration. Suresh et al. [20] prepared  $\text{Al}_2\text{O}_3$ -Cu hybrid nanofluids with varying volume concentration of 0.1–2% with sodium lauryl sulfate as a dispersant. Authors concluded that an increase in volume concentration of nanoparticles leads to an increase in the thermal conductivity of the nanofluids. The thermo-

physical properties of the Ag-MgO/water hybrid nanofluids were studied by Esfe et al. [21] and proposed the theoretical models for thermal conductivity and viscosity for the hybrid nanofluids. The results of developed theoretical models were found in good agreement with experimental results at low volume concentration. Madhesh et al. [22] studied convective heat transfer analysis of Cu-TiO<sub>2</sub> hybrid nanofluids in the tube-type heat exchanger. They found that the convective heat transfer coefficient was enhanced by 68% using hybrid nanofluids ( $\phi = 1\%$ ). Apart from the thermal conductivity, Yarmand et al. [23] investigated other important properties such as density, specific heat, and viscosity of graphene nanoplatelet/platinum hybrid nanofluids. The qualitative investigation of these properties is important for the calculation of heat transfer enhancement in the synthesis of hybrid nanofluids. Low-cost hybrid nanofluid containing nanocomposite of biomass carbon/graphene oxide was prepared by Yarmand et al. [24] and its thermo-physical properties were studied. The key literature is summarized in Tables 1 and 2 [25–30]. Recently, Esfe et al. [31] has carried out a price performance analysis of hybrid nanofluids in consideration with thermal conductivity. Authors concluded that for improved heat transfer of hybrid nanofluids, the extra cost needs to be paid for synthesis process.

It is evident from the literature that, most of hybrid nanofluid synthesis methods did not have proper stability due to uneven mixing or irregular coating of nanoparticles over other nanoparticles surface. These uneven mixing or irregular coating of nanoparticles leads to improper stability, and it limits the enhancement in thermal properties. In view of this, the high-thermal-conductivity nanoparticles (metallic and carbon based) can be uniformly coated on the surface of the low-thermal-conductivity nanoparticles (metal oxides) for improving its thermal performance. The present study reports the comparative study of thermo-physical properties of water-based ZnO and Ag/ZnO hybrid nanofluids. The efforts have been taken to coat Ag nanoparticles uniformly over ZnO nanoparticles by wet chemical methods. Literature review concludes that no study has been reported on the synthesis and thermo-physical properties of water-based Ag/ZnO hybrid nanofluids.

## Synthesis of water-based ZnO and Ag/ZnO nanofluids

The nanofluids were prepared by the two-phase method. In the initial phase, the ZnO and Ag/ZnO nanoparticles were synthesized by the wet chemical method. In the next phase, the prepared nanoparticles were dispersed in base fluid (DI water) to get the desired nanofluids of different volume concentration ranging from 0.02 to 0.1%.

**Table 1** Summary of thermal conductivity enhancement in hybrid nanofluids

Author(s)	Hybrid nanoparticles synthesis method	Base fluid	Thermal conductivity (TC) enhancement
Yarmand et al. [16]	Graphene + Ag chemical vapor deposition	Water	Enhancement in TC was 22.22% at 0.1% mass concentration for 40 °C
Baby et al. [17]	CuO + graphene (reduction method)	Water and EG	Enhancement in TC was ~ 28% at 0.05% volume concentration for 25 °C
Munkhbayar et al. [18]	Ag + MWCNT (pulse power evaporation)	Water	Enhancement in TC was 14.5% at 3% mass concentration for 40 °C
Tadjarodi et al. [19]	Ag + silica (reduction method)	Glycerol	Enhancement in TC was 10.95% at 4% Silica and 2.98% Ag mass concentration for 25 °C
Suresh et al. [20].	Al <sub>2</sub> O <sub>3</sub> + Cu (thermo-chemical synthesis)	Water	Enhancement in TC was 12.11% at 2% volume concentration
Hemmat Esfe et al. [21]	ZnO + DWCNT (mixed)	Water and EG	Enhancement in TC was ~ 32% at 1% volume concentration for 50 °C
Madhesh et al. [22]	Cu + TiO <sub>2</sub> (milling)	Water	Enhancement in TC was ~ 9% at 2% volume concentration for 45 °C
Yarmand et al. [23]	Graphene + platinum (chemical reaction)	Water	Enhancement in TC was ~ 17.77% at 0.1% mass concentration
Yarmand et al. [24]	Biomass carbon/graphene oxide (mixed)	EG	Enhancement in TC was ~ 6.67% at 0.06% mass concentration for 40 °C
Syam Sundar et al. [25]	MWCNT + Fe <sub>2</sub> O <sub>3</sub> (chemical co-precipitation)	Water	Enhancement in TC was ~ 21% at .3% volume concentration for 40 °C
Esfe et al. [26]	Ag + MgO (mixed)	Water	Enhancement in TC was ~ 20% at 0.02% volume concentration
Toghraie et al. [28]	ZnO-TiO <sub>2</sub> /EG	EG	Enhancement in TC was 22% at 0.96% mass concentration for 50 °C
Masoud Zadkhast et al. [29]	MWCNT-CuO/water	Water	Enhancement in TC was 30.38% at 0.6% mass concentration for 50 °C
Esfe et al. [30].	MWCNT/SiO <sub>2</sub> (mixed)	Water + EG	Enhancement in TC was 32% at 3.5% mass concentration for 50 °C

**Table 2** Summary of viscosity enhancement in hybrid nanofluids

Author(s)	Hybrid nanoparticles synthesis method	Enhancement in viscosity
Yarmand et al. [16]	Graphene + Ag chemical vapor deposition	Enhancement in viscosity was 30% at 0.1% mass conc. at 40 °C
Tadjarodi et al. [19]	Ag + silica (reduction method)	Enhancement in viscosity was 54% at 4% mass conc. at 20 °C
Suresh et al. [20]	Al <sub>2</sub> O <sub>3</sub> + Cu (thermo-chemical synthesis)	Enhancement in viscosity was 115% at 2% volume conc.
Yarmand et al. [23]	Graphene + platinum chemical reaction	Enhancement in viscosity was 1.33 times of water at 0.1% mass conc. at 40 °C
Yarmand et al. [24]	Biomass carbon/graphene oxide (mixed)	Enhancement in viscosity was 4.16% at 0.06% mass conc. at 20 °C
Syam Sundar et al. [25]	MWCNT + Fe <sub>2</sub> O <sub>3</sub> (chemical co-precipitation)	Enhancement in viscosity was 1.5 times of water at 3% volume conc. at 60 °C

## Chemicals and materials

The primary chemicals utilized in the preparation are zinc salt [ $\text{Zn}(\text{NO}_3)_2 \cdot 6\text{H}_2\text{O}$ , molecular weight =  $297.49 \text{ gm mol}^{-1}$ ], silver nitrate [ $\text{AgNO}_3$ , molecular weight =  $169.87 \text{ g mol}^{-1}$ ], polyvinyl alcohol [molecular weight =  $96800 \text{ g mol}^{-1}$ , degree of polymerization of 2000], ammonium hydroxide [ $\text{NH}_4\text{OH}$ ], sucrose [ $\text{C}_{12}\text{H}_{22}\text{O}_{11}$ , molecular weight =  $342.30 \text{ g mol}^{-1}$ , 99.95% pure]. The chemicals, namely zinc salt and silver nitrate, were procured from Sigma-Aldrich, USA. The ammonia solution and sucrose were procured from Merck, USA, and polyvinyl alcohol (The Fischer Scientific) in the solid form. All chemicals and materials which have been used in the synthesis of ZnO and Ag/ZnO have purity more than 99.90%. The schematic representation of the synthesis of Ag/ZnO nanoparticles is described in Fig. 1.

## Synthesis of ZnO and Ag/ZnO nanoparticles

In a systematic synthesis process, a continuous magnetic stirring of the aqueous PVA/sucrose solution (taken in a ratio of 1:10 by mass) was performed for 24 h. After 24 h, PVA/sucrose solution was heated up to  $60\text{--}65 \text{ }^\circ\text{C}$  followed by dropwise addition of aqueous solution of  $\text{Zn}^{2+}$  salt (0.2 M concentration) into PVA/sucrose solution. The pH of the reaction mixture was kept constant (approximately 9) by supplying the required amount of  $\text{NH}_4\text{OH}$  solution to balance the addition of hydrogen in  $\text{Zn}^{2+}$  cations. After the completion of the reaction, the mixture was maintained at  $25 \text{ }^\circ\text{C}$  for a 24-h period before gradually pouring out the clear and colorless top portion of the polyvinyl alcohol/sucrose solution. Eventually, the acquired solution was thoroughly washed with methanol followed by drying at a temperature of about  $50\text{--}60 \text{ }^\circ\text{C}$  to acquire the white mass of polymer-capped ZnO/precursor powders. Recrystallized pristine ZnO nanoparticles were acquired after heating the synthesized polymeric precursor powder at  $400\text{--}500 \text{ }^\circ\text{C}$  in a furnace for a duration of 2 h.

For the preparation of Ag-coated ZnO nanoparticles, the dried ZnO precursor powder (5.0 g by mass) was mixed in an aqueous solution of silver nitrate with 0.25 M concentration and 100 mL quantity under continuous magnetic stirring at  $50\text{--}60 \text{ }^\circ\text{C}$  in darkness. After 20–30 min of reaction, the powders were recovered by gradually pouring out the  $\text{AgNO}_3$  mixture and subsequent cleaning in hot water and dehydrating at a relatively lower pressure (10–100 mbar) environment at  $20\text{--}25 \text{ }^\circ\text{C}$ . Eventually, the dehydrated powders were heated between 400 and  $500 \text{ }^\circ\text{C}$  for a time period of 2 h in ambient air. The recrystallized ZnO nanoparticles so acquired are now capped with a thin and uniform shell layer of Ag. This synthesized Ag/ZnO nanoparticles can be used to prepare nanofluids.

## Preparation of ZnO and Ag/ZnO nanofluids

The use of nanofluids in heat transfer applications depends on methods of synthesis, long-term stability, surfactant-free stabilization, improved heat transfer capacity, and low viscosity which reduces pumping power in case of active heat transfer devices. The stability of nanofluids extensively depends upon factors like surface energies of the nanoparticles, van der Waals forces, and Brownian motion of nanoparticles in the base fluid. More surface charge on the particles results in the instability and agglomeration of the nanoparticles which leads to a decrease in heat transfer capacity of nanofluids [32]. In addition, the high concentration of nanoparticles in base fluid is restricted because it leads to agglomeration and increase in viscosity. The ZnO and Ag/ZnO are highly dense nanoparticles. Thus, stabilization of these particles becomes difficult at high concentration. Taking a hint from the literature, the different concentrations selected to study the stability and thermo-physical properties are varied at volume concentration from 0.02, 0.04, 0.06, 0.08, and 0.1% (for both ZnO/water and Ag/ZnO/water nanofluids). In the present study, the nanofluids were synthesized with the use of deionized water (DI) as a base fluid by a two-step method. The ZnO/water nanofluids were prepared by adding an acetyl-acetone surfactant (Fig. 2a). Water-based ZnO nanofluids stability is one of the

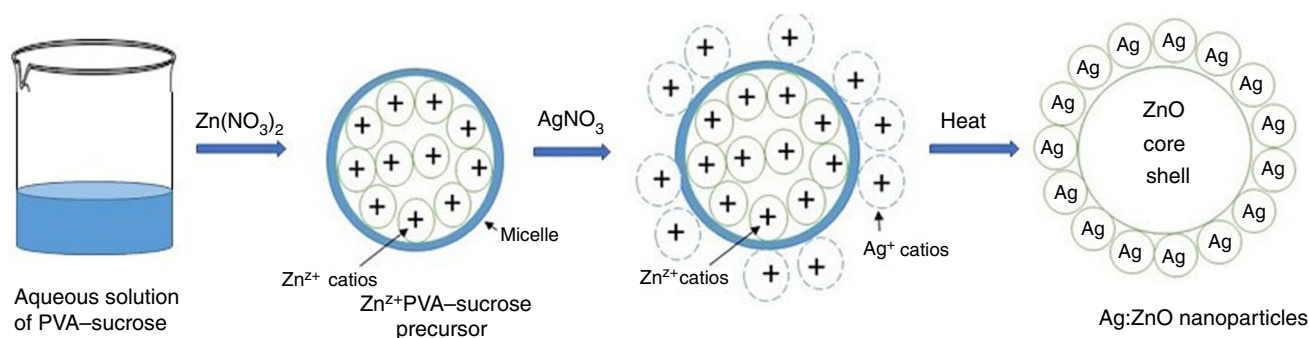


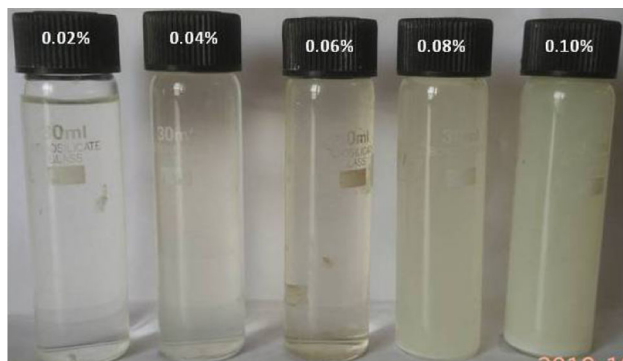
Fig. 1 Schematic representation of the synthesis of Ag/ZnO nanoparticles

challenges and which is discussed by previous research [8]. However, in case of Ag/ZnO nanoparticles, the outer surface of ZnO becomes hydrophilic in nature that helps in making nanofluids without any surfactant. However, due to the high density of Ag/ZnO nanoparticles, the stability of the nanofluids is the issue. This issue was solved by sonicating the nanofluids for about 5 h. Figure 2b shows the nanofluids at different volume concentration. The addition of surfactant during nanofluids synthesis may change the thermo-physical characteristics of base fluids. The amount of nanoparticles required for a varied range of volume concentration is calculated by using Eq. (1). The surfactant-free Ag/ZnO nanofluids is the main focus of the study which is reported in the next section.

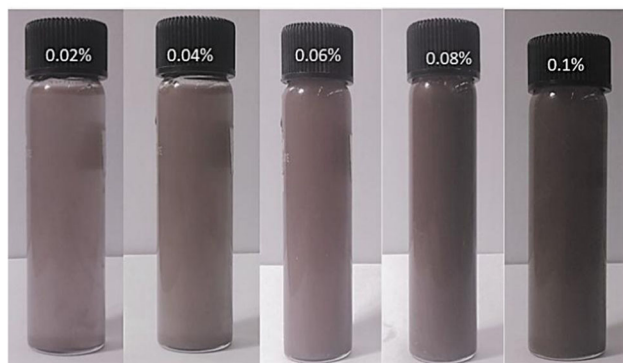
$$\phi = \frac{\frac{m_n}{\rho_n}}{\frac{m_b}{\rho_b} + \frac{m_n}{\rho_n}} \quad (1)$$

### Characterization of ZnO and Ag/ZnO nanoparticles and thermo-physical properties measurement of nanofluids

The morphology of the ZnO and Ag/ZnO nanoparticles were observed and studied with a field emission scanning



(a)



(b)

**Fig. 2** Images of **a** ZnO nanofluids, **b** Ag/ZnO nanofluid at a different volume concentration

electron microscope (FESEM Carl Zeiss SUPRA 55). The elemental constitution was also observed and studied with energy-dispersive spectrometer (EDS) equipped with the FESEM. The crystalline nature and phase purity of the samples were observed and studied with an X-ray diffraction machine by use of  $\text{CuK}_\alpha$  radiation of wavelength 0.1545 nm (PANalytical X'Pert Pro). The average hydrodynamic nanoparticles diameter measured by dynamic light-scattering (DLS) technique for nanofluids (ZnO and Ag/ZnO). The zeta potential value was reported to confirm the stability of various nanofluids.

To understand and study the performance and behavior of nanofluids for heat transfer, two important thermo-physical characteristics, namely thermal conductivity and viscosity, were measured. The transient hot-wire method was used to measure the thermal conductivity of liquids to avoid natural convection effects during measurement. In this view, KD2 Pro thermal property analyzer (Model: KD2 Pro., Make: Decagon Device, USA) was used to measure the thermal conductivity property of Ag/ZnO nanofluids. The KD2 Pro thermal property analyzer meets both ASTM D5334 and IEEE442-1981 standard. The principle behind this measurement is that it measures time-temperature response by transient hot wire to an electrical impulse. Targeted prototypes thermal conductivity is sensed by the thermal temperatures variation for a specified time interval. As it is temperature dependent, the measurements were taken at different temperature variations (20–45 °C). The targeted sample is filled in the 45-mL sealed tube in which the sensor is dipped. At the time of measurement for maintaining a constant temperature, the sample is allowed to stabilize for some time.

The measurement of viscosity is very important as pumping cost increases with an increase in viscosity. In this work, the viscosity was measured by cone and plate viscometer (model Brookfield DVII + Pro, make Brookfield digital viscometer, USA). The cone is connected to the spindle drive, while the plate is mounted on the sample cup. The spindle (CPE-40) is used in this study and can be used for measuring the viscosity in the range 0.015–3065 cP. The viscometer consists of a cone of angle 0.080° and 2.4 cm length attached to the spindle drive. When the spindle rotates, it measures the viscous force of fluid against the spindle by the deviation of the calibrated spring.

## Results and discussion

The synthesized ZnO and Ag/ZnO nanoparticles were characterized by different characterization methods viz. scanning electron microscopy (SEM) and X-ray diffraction (XRD). In the successive step, the nanofluids of ZnO and

Ag/ZnO were prepared with varied volume concentration ( $\phi = 0.02\text{--}0.1\%$ ). The stability and thermo-physical properties of the prepared nanofluids were measured. The observations obtained from the present investigation are summarized below.

### Structural properties of the ZnO and Ag/ZnO nanoparticles

Figure 3 shows the X-ray diffraction patterns of (1) the ZnO nanoparticles after heating the precursor at a temperature of 500 °C, (2) Ag-treated ZnO polymer precursor powder and (3) Ag-coated ZnO nanoparticles after heating at 500 °C for a time duration of 2 h. Figure 3 depicts the X-ray diffraction pattern of ZnO nanoparticles with eleven expansive and well-defined peaks in the diffraction angle range of 20°–80°, corresponding to the wurtzite-type crystal structure of ZnO (JCPDS#036-1451-space group *P63mc*). The X-ray diffraction pattern of the Ag-coated ZnO precursor shows four well-defined peaks analogous to the metallic Ag of *face-centered-cubic* crystal structure (JCPDS#04-0783) and two weakened peaks analogous to cubic silver oxide (JCPDS#04-013-0189). This affirms that the  $\text{Zn}^{2+}$ -polyvinyl alcohol-sucrose precursor powders act as a soft template for the growth of silver ions on ZnO. The X-ray diffraction pattern of Ag-coated ZnO nanoparticles heated at 500 °C consist of nine distinct peaks of wurtzite-type ZnO along with the four intense and wide peaks of *face-centered-cubic* Ag in the  $2\theta$  range of 20°–80°. No traces of AgO can be seen in this recrystallized Ag-coated ZnO nanoparticles powder. It confirms the formation of Ag-coated ZnO heterostructure. The mean size of ZnO crystallites ( $d_{\text{DS-ZnO}}$ ) in the pure and Ag/ZnO nanoparticles heated at 500 °C is 15 and 20 nm, respectively. Similar

values are predicted from the full width at half maxima (FWHM) values of the X-ray diffraction peaks and Debye-Scherrer's formula. In a similar way, mean size of silver crystallites ( $d_{\text{DS-Ag}}$ ) is calculated and observed to be 18 and 25 nm in the Ag-coated precursor powders and the Ag/ZnO sample processed at 500 °C, respectively. Rietveld investigation of the ZnO peaks gives the lattice parameters,  $a = 0.3252$  nm,  $c = 0.5215$  nm,  $c/a = 1.6036$ , and unit cell volume ( $V_0$ ) =  $47.76 \times 10^{-3}$  nm<sup>3</sup> in ZnO nanoparticles heated at 500 °C, as compared to the values of  $a = 0.3257$  nm,  $c = 0.5226$  nm,  $c/a$  ratio is observed to be 1.6045 and  $V_0 = 48.02 \times 10^{-3}$  nm<sup>3</sup> in Ag-coated ZnO nanoparticles heated at same temperature. The *fcc* Ag (*Fm3m* space group) peaks show the values  $a = 0.4087$  nm, and  $V_0 = 68.27 \times 10^{-3}$  nm<sup>3</sup> for the samples derived at 500 °C, correlated to the values of  $a = 0.4086$  nm and  $V_0 = 68.22 \times 10^{-3}$  nm<sup>3</sup> in bulk Ag (JCPDS card: 04-0783). These results throw light upon the renovation of the surface of ZnO nanoparticles. The preparation procedure is very compelling in acquiring Ag coating through the soft base template of a polymeric precursor of ZnO.

The surface morphology of ZnO and Ag/ZnO nanoparticles has been studied using SEM images depicted in Fig. 4a–e. Figure 4a–c shows loose agglomerates of ZnO and Ag/ZnO nanoparticles in the micrographs. The magnified view reveals that the nanoparticles have grown bigger in size by forming clusters up to 500 nm–1  $\mu\text{m}$ . The Ag/ZnO nanoparticles show flower-like morphologies and ZnO nanoparticles show hexagonal structure (Fig. 4d–e). A closer observation of the magnified images indicates that these clusters consist of the well-organized group of flower petal-like structure along the axial development of the clusters (perpendicular to the plane of the image), and the petal-like structures are stretched out in a radial direction from the hexagonal faces of the cluster assembly. Each of these petal-like structures can be distinguished as a cluster of tiny Ag-coated ZnO nanoparticles. A closer view shows that ZnO nanoparticles has hexagonal platelet size less than 100 nm and residing with one another in the assembly of facet structures (Fig. 4e). Figure 4f shows the elemental composition of the synthesized Ag/ZnO nanoparticles calcinated at 500 °C. A quantitative measurement shows an atomic content of 34.81% zinc, 61.05% oxygen, and 4.14% silver.

### Stability of the nanofluids

The stability of nanofluids has its own importance to decide the nanofluids thermo-physical properties. Many authors reported several methods to analyze the stability of the nanofluids such as spectral analysis, zeta potential, and dynamic light-scattering methods. In this study, stability

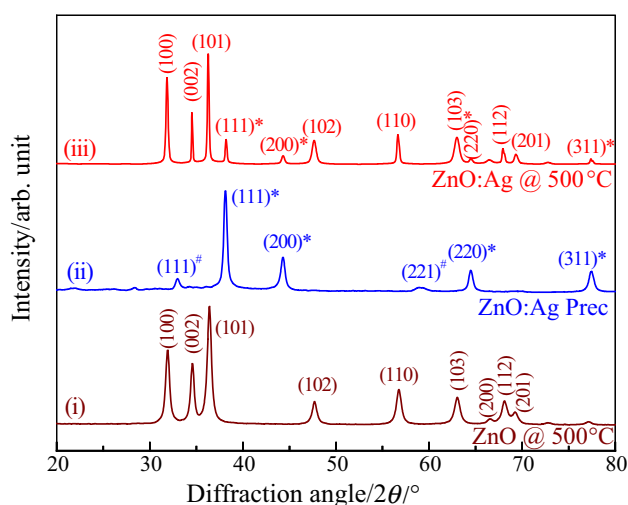
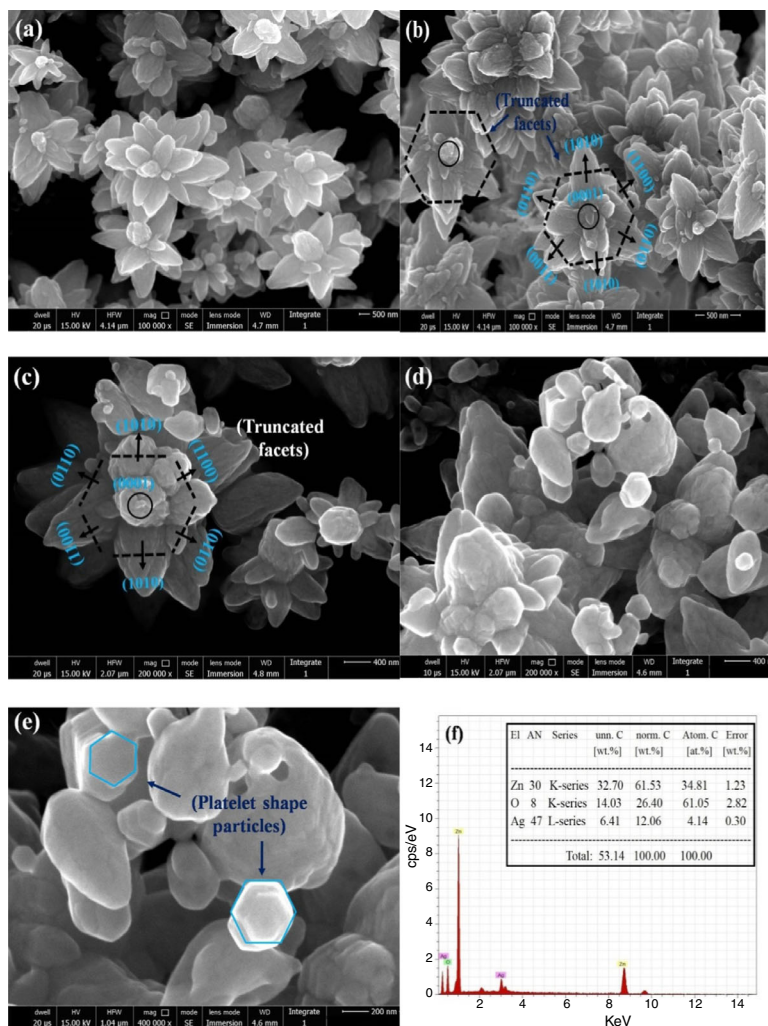


**Fig. 3** X-ray diffraction peaks for (i) ZnO at 500 °C, (ii) Ag/ZnO precursor, (iii) Ag/ZnO at 500 °C nanoparticles

**Fig. 4** FESEM images: **a, b** Ag/ZnO nanoparticles at magnification of  $\times 100,000$ , **c** Ag/ZnO nanoparticles at magnification of  $\times 200,000$ , **d** ZnO nanoparticles magnification of  $\times 200,000$ , **e** ZnO nanoparticles magnification of  $\times 400,000$ , **f** EDS spectrum of Ag/ZnO



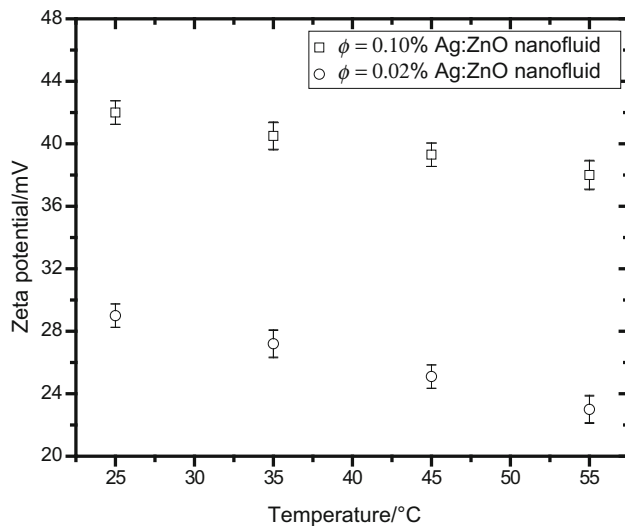
has been analyzed using zeta potential test (model Nano-ZS, make Malvern Instrument, UK). The electrostatic repulsion is considered as the mechanism to stabilize the colloidal suspensions. These repulsive forces are sufficiently strong to overcome the attractive forces caused by van der Waals forces. Zeta potential is the measure of the repulsive forces between particles. According to the stabilization theory, the electrostatic repulsion between the particles increases if the zeta potential has higher absolute value. This may be due to the fact that at a higher surface charge, the repulsion between the particles increases resulting in lesser agglomeration [33]. It is argued that the suspension exhibits good stability if the zeta potential value is higher than 30 mV. The measured value of the zeta potential at room temperature (25 °C) for varying concentration ( $\phi = 0.02\text{--}0.1\%$ ) of Ag/ZnO nanofluids are summarized in Table 3. It is also observed that the zeta potential decreases with increase in volume concentration. The increase in volume concentration increases in agglomeration among the nanoparticles which lead to a

lower value of zeta potential. The variation in zeta potential with temperature is depicted in Fig. 5. The increase in temperature accelerates agglomeration which leads to higher average hydrodynamic sizes and lower value of zeta potential. At high temperatures, the velocity or kinetic energy is high enough to overcome the Van der Waals forces, and it destabilizes the nanofluids. Similar observations also reported in the past literature [34].

The dynamic light-scattering (DLS) test was performed to determine the particles size distribution and mean particle size of the nanoparticles in nanofluids. In this method, a continuous-wave laser beam (632.8 nm range) passes through a colloidal suspension of a given sample and the particles in the suspension scatter some of the light in all direction (Rayleigh scattering). This is due to smaller particle size compared to the laser wavelength. In addition, the small particles in the suspension move randomly resulting in fluctuation in the scattered light in the detector plane. This fluctuation is related to the diffusion rate of the

**Table 3** Zeta potential values at different concentration

Zeta potential value/mV	Volume concentration ( $\phi$ )/%
42	0.02
39	0.04
37	0.06
34	0.08
29	0.1

**Fig. 5** Effect of temperature on the zeta potential

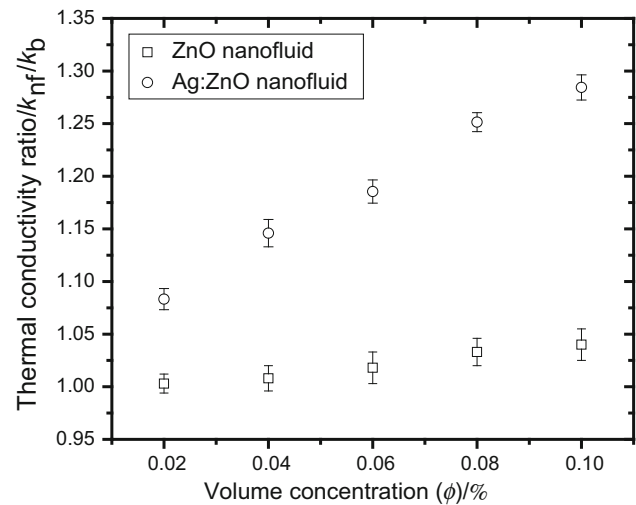
particles, and the diffusion coefficient of the particles is given by [33],

$$D_c = \frac{K_B T}{6\pi\mu r} \quad (2)$$

The average hydrodynamic diameters for Ag/ZnO nanofluids with 0.02% and 0.1% volume concentration was found to be in the range of 96 nm and 125 nm, respectively. It is observed that, at higher particles volume concentrations, nanoparticles agglomerate due to strong inter particles interaction resulting sedimentation of the nanofluids. On the contrary, lower nanoparticles concentration reduces the interparticle interaction and enhances the stability.

### Thermal conductivity and viscosity of nanofluids

In this study, the effective thermal conductivity of the nanofluids was measured by using the thermal property analyzer (model KD2 Pro., make Decagon Device, USA) with isothermal bath. The sensor needle (KS-1) used during measurement was made up of stainless steel with 6 cm

**Fig. 6** Enhancement in the thermal conductivity of ZnO nanofluids by a coating of Ag

long and 0.13 cm in diameter. The calibration of the sensor needle was carried out by measuring the thermal conductivity of various known fluid such as DI water and glycerin. The measured thermal conductivities for distilled water and glycerin are found  $0.63 \text{ W m}^{-1} \text{ K}^{-1}$  and  $0.292 \text{ W m}^{-1} \text{ K}^{-1}$ , respectively. The sensor needle can be used to measure the thermal conductivity of the fluids in the range of  $0.02\text{--}2 \text{ W m}^{-1} \text{ K}^{-1}$  with an accuracy of  $\pm 5\%$ .

Figure 6 depicts the variation in thermal conductivity for ZnO and Ag/ZnO nanofluids at 25 °C. The thermal conductivity of Ag/ZnO nanofluids is found higher compared to ZnO nanofluids at each concentration. The maximum value of thermal conductivity for Ag/ZnO nanofluid is found to be 20% and 28% when they compared with ZnO nanofluid and water, respectively. The coating of Ag nanoparticles by wet chemical method helps for uniform covering of Ag nanoparticles over ZnO micelle (Fig. 4c) which leads to improving the stability of nanoparticles. The increase thermal conductivity of Ag/ZnO nanofluid is combined effect of increased stability and higher thermal conductivity coating of Ag nanoparticles over ZnO nanoparticles. The temperature variation for thermal conductivity at varying concentration of ZnO nanofluids is shown in Fig. 7a. It is observed that the thermal conductivity of the ZnO nanofluids increases with increase in temperature. The increase in temperature promotes Brownian motion among nanoparticles, which leads to an increase in thermal conductivity. The maximum thermal conductivity of the ZnO nanofluid found to be 8.0% at 45 °C (for  $\phi = 0.1\%$ ). The ZnO nanoparticles are hydrophobic in nature and not easily disperse in water. Many researchers prepared water-based ZnO nanofluid with different surfactant addition methods at low volume



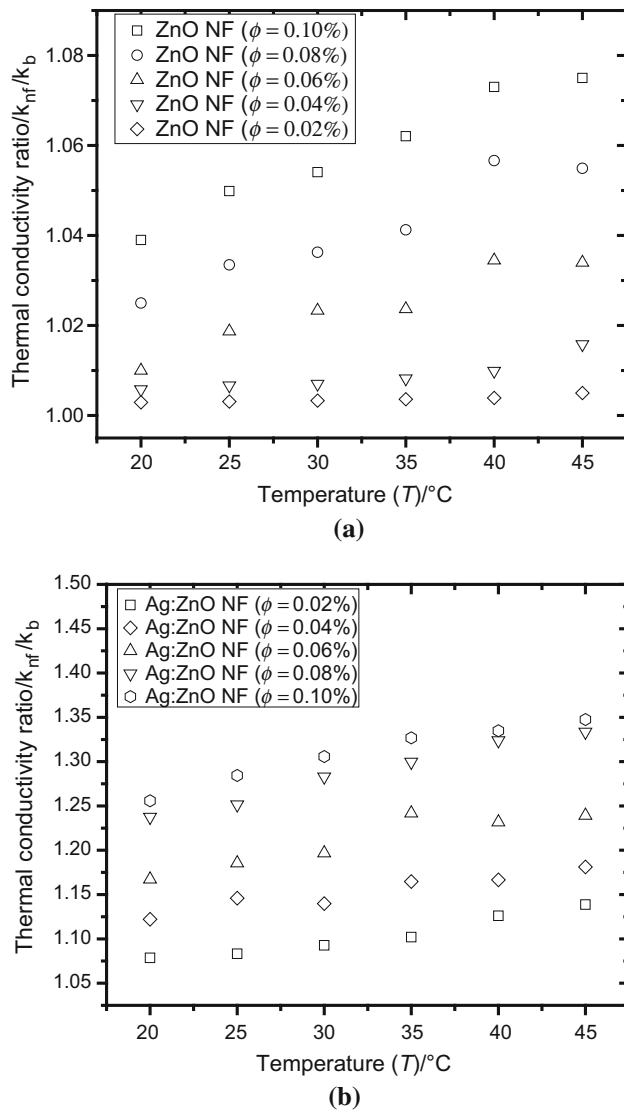


**Fig. 7** Effective thermal conductivity of **a** ZnO with varying temperature at 0.02–0.1% volume concentration. **b** Ag/ZnO with varying temperature at 0.02–0.1% volume concentration

concentration [8]. The amount of surfactant required for proper stability of nanofluid increases with increase in concentration. The higher amount of surfactant may lead to change in thermo-physical properties because of agglomeration of the nanoparticles [8].

Most of the recent work focused on the synthesis of hybrid nanofluid to improve the thermal properties by mixing low-thermal-conductivity nanoparticles with high-thermal-conductivity nanoparticles [18, 21]. Present research work involves uniform coating of highly conductive Ag nanoparticles on ZnO nanoparticles where Ag get bonded firmly on the periphery of ZnO nanoparticles. Figure 7b shows enhancement in thermal conductivity of the Ag/ZnO nanoparticles dispersed in water with temperatures and at varying concentration. The increase in

thermal conductivity can be defined in different ways. Firstly, the addition of nanoparticles in the base fluid decreases the mean free path between the adjacent particles and enhances the Brownian motion. Secondly, the increase in the Brownian motion of the nanoparticles helps to shoot up the lattice vibration between the molecules. In addition to Brownian motion, high-thermal-conductivity nanolayer (Ag) is formed in case of Ag/ZnO nanofluids. This nanolayer is a coating of highly thermally conductive Ag metal on ZnO nanoparticles. The uniform coating shown in FESEM images (Fig. 4a–c) helps to improve the surface properties of ZnO nanoparticles, which is a feasible condition for increased thermal conductivity and stability. In addition, uniform coating of Ag makes ZnO nanoparticles more hydrophilic in nature which leads to enhancing the stability of nanofluid because of proper dispersion of nanoparticles in water base fluids. The proper stability is one of the reasons for enhanced thermal conductivity. Also, the result shows that the trends of variation in increase in the thermal conductivity of Ag/ZnO nanofluids with temperature are found similar to ZnO nanofluids, but in case of Ag/ZnO nanofluids, trends are more inclined (Fig. 7a, b).

The viscosity of the fluid is the measure of its resistance to deformation. In case of flow through ducts, the pressure drop and the pumping power requirement depends on the viscosity of the fluid, although the nanofluid increases the heat transfer performance. These fluids exhibit an enhancement in the viscosity compared to the base fluid. The viscosity of the nanofluid depends on the particle shape, particles size, volume fraction, and temperature of the nanofluid. In present work, the efforts have been made to study the effects of the temperature and the nanoparticles concentration on viscosity. The calibration of the viscometer was carried out by measuring the viscosity of various known fluids such as DI water and glycerin. The measured viscosity values for distilled water and glycerin are found 0.00083 and 0.0109 Pa s, respectively. The results agree well with the literature value of 0.00079 and 0.0107 Pa s for water and glycerin with an accuracy of  $\pm 5\%$ . Figure 8 depicts the viscosity of ZnO nanofluids at varying concentration ( $\phi = 0.02$ –0.1%). The viscosity of both the nanofluids increases with increase in nanoparticles concentration in base fluids. The agglomeration and clustering are the reasons for the enhanced viscosity of nanofluids. The clustering of nanoparticles in base fluid promotes heat transfer in certain conditions [35]. On one hand, clustering should be in limit; otherwise, it leads to agglomeration. The trend of viscosity variation at different concentration of nanoparticles for ZnO and Ag/ZnO nanofluids if found to be similar. The Ag/ZnO nanofluids show a negligible increase in viscosity when it compared with results of the viscosity of ZnO nanofluids. For the various heat transfer applications, flow properties of the

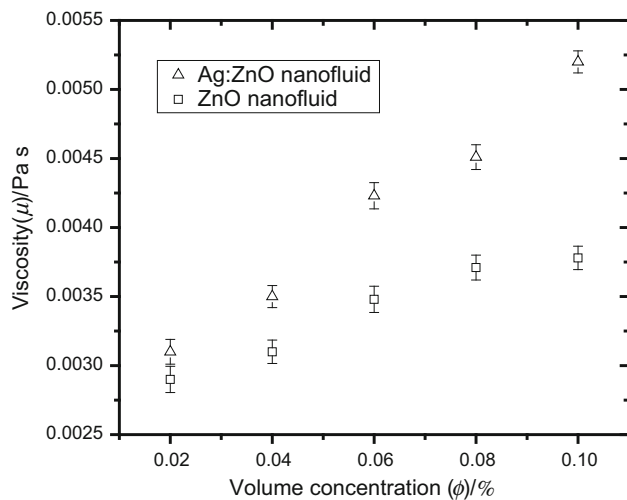


**Fig. 8** Viscosity of ZnO and Ag/ZnO nanofluids at different concentrations

nanofluids are very essential. In addition to that, clustering and agglomeration also affect the heat transfer. In this case, the heat transfer process can be view as a function of viscosity, which describes resistance to the flow and also function of temperature. For the same reason, the dynamic viscosity of different concentration of ZnO and Ag/ZnO at a constant shear rate as was measured as a function of the temperature (20–40 °C) is shown in Fig. 9a, b. The dynamic viscosity of the nanofluids increases with increase in the concentration of nanoparticles and decreases with increase in temperature. For all concentration of the ZnO nanofluids, change in viscosity with respect to temperature shows linear behavior.

## Conclusions

In this study, two different nanoparticles namely, ZnO and Ag/ZnO have been synthesized by the wet chemical method. The materials characterization techniques such as FESEM, X-ray diffraction method, and EDS utilized to confirm surfaces morphology, elemental composition, and particle size. After successful synthesis and characterization of nanoparticles, the water-based nanofluids namely ZnO and Ag/ZnO were prepared with varying concentration ( $\phi = 0.02$ – $0.1\%$ ). The stability and thermo-physical properties for nanofluids were measured and studied with different parameters (concentration and temperature). The conclusions of the above study are elaborated:

(1) The surface morphology confirms hexagonal-shaped structures for ZnO nanoparticles and the petal-like structures for Ag/ZnO hybrid nanoparticles (Ag stretched out in a radial direction from the hexagonal faces of the ZnO nanoparticles).

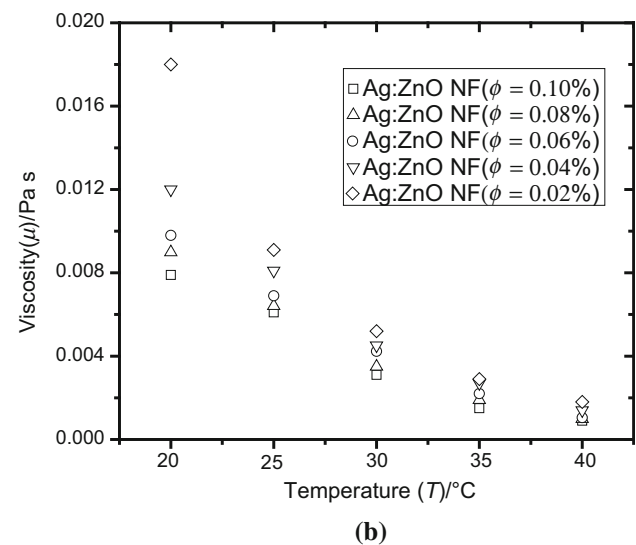
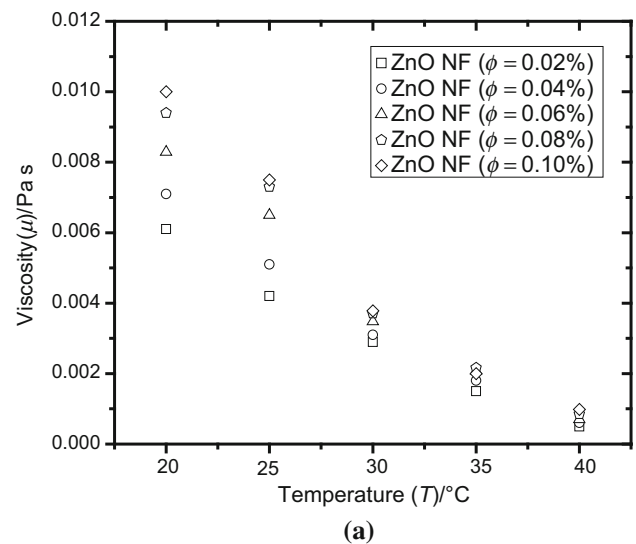


**Fig. 9** Viscosity as a function of temperature for: **a** ZnO nanofluids, **b** Ag/ZnO oxide nanofluids

- (2) The average crystallite size for Ag/ZnO nanoparticles found to be 25 nm. X-ray diffraction patterns revealed the presence of the uniform coating of Ag over the ZnO nanoparticles.
- (3) The average hydrodynamic diameters for Ag/ZnO nanofluids with 0.02% and 0.1% volume concentration was found to be in the range of 96 nm and 125 nm. The stability of nanofluids was measured by zeta potential test. The prepared nanofluids are found to be stable and its corresponding zeta potential values are in the range of 29–42 mV.
- (4) The thermal conductivity of Ag/ZnO nanofluids is found to be higher when it is compared to ZnO nanofluids. The maximum thermal conductivity enhancement for Ag/ZnO nanofluids are found to

20% and 28% when it compared with ZnO nanofluids and water, respectively.

- (5) The uniform coating of higher thermal conductivity materials (Ag) over metallic oxides (ZnO) causes an increase in thermal conductivity. In addition, uniform coating of Ag makes ZnO nanoparticles more hydrophilic in nature which leads to enhanced stability of nanofluids because of proper dispersion of nanoparticles in water base fluids. The good stability is one of the reasons for enhancement in thermal conductivity. These two important fact leads to the use of hybrid Ag/ZnO nanofluids for heat transfer applications.
- (6) The thermal conductivity of nanofluids increases with increase in temperature for both ZnO and Ag/ZnO nanofluids.
- (7) The Ag/ZnO nanofluids show a negligible increase in viscosity when it compared with results of the viscosity of ZnO nanofluids.

## References

1. Modak M, Srinivasan S, Garg K, Chougule SS, Agarwal MK, Sahu SK. Experimental investigation of heat transfer characteristics of the hot surface using  $\text{Al}_2\text{O}_3$ -water nanofluids. *Chem Eng Process Process Intensif*. 2015;91:104–13. <https://doi.org/10.1016/j.cep.2015.03.006>.
2. Modak M, Chougule SS, Sahu SK. An experimental investigation on heat transfer characteristics of hot surface by using CuO-water nanofluids in circular jet impingement cooling. *J Heat Transf*. 2017;140:012401. <https://doi.org/10.1115/1.4037396>.
3. Chougule SS, Sahu SK. Heat transfer and friction characteristics of  $\text{Al}_2\text{O}_3$ /water and CNT/water nanofluids in transition flow using helical screw tape inserts—a comparative study. *Chem Eng Process Process Intensif*. 2015;88:78–88.
4. Putra N, Yanuar IFN. Application of nanofluids to a heat pipe liquid-block and the thermoelectric cooling of electronic equipment. *Exp Therm Fluid Sci*. 2011;35:1274–81. <https://doi.org/10.1016/j.expthermflusci.2011.04.015>.
5. Choi SUS, Eastman JA. Enhancing thermal conductivity of fluids with nanoparticles. *ASME Int Mech Eng Congr Expos*. 1995;66:99–105. <https://doi.org/10.1115/1.1532008>.
6. Chandrasekar M, Suresh S, Bose AC. Experimental investigations and theoretical determination of thermal conductivity and viscosity of  $\text{Al}_2\text{O}_3$ /water nanofluid. *Exp Therm Fluid Sci*. 2010;34:210–6. <https://doi.org/10.1016/j.expthermflusci.2009.10.022>.
7. Saeedinia M, Akhavan-Behabadi MA, Razi P. Thermal and rheological characteristics of CuO-Base oil nanofluid flow inside a circular tube. *Int Commun Heat Mass Transf*. 2012;39:152–9.
8. Raykar VS, Singh AK. Thermal and rheological behavior of acetylacetone stabilized ZnO nanofluids. *Thermochim Acta*. 2010;502:60–5. <https://doi.org/10.1016/j.tca.2010.02.007>.
9. Saleh R, Putra N, Wibowo RE, Septiadi WN, Prakoso SP. Titanium dioxide nanofluids for heat transfer applications. *Exp Therm Fluid Sci*. 2014;52:19–29. <https://doi.org/10.1016/j.expthermflusci.2013.08.018>.
10. Kulkarni DP, Namburu PK, Ed Bargar H, Das DK. Convective heat transfer and fluid dynamic characteristics of  $\text{SiO}_2$ -ethylene glycol/water nanofluid. *Heat Transf Eng*. 2008;29:1027–35.
11. Parametthanuwat T, Bhuwaketkumjohn N, Rittidech S, Ding Y. Experimental investigation on thermal properties of silver nanofluids. *Int J Heat Fluid Flow*. 2015;56:80–90. <https://doi.org/10.1016/j.ijheatfluidflow.2015.07.005>.
12. Riehl RR, Dos SN. Water-copper nanofluid application in an open loop pulsating heat pipe. *Appl Therm Eng*. 2012;42:6–10. <https://doi.org/10.1016/j.applthermaleng.2011.01.017>.
13. Chougule SS, Sahu SK. Thermal performance of automobile radiator using carbon nanotube-water nanofluid-experimental study. *J Therm Sci Eng Appl*. 2014;6:041009. <https://doi.org/10.1115/1.4027678>.
14. Meriläinen A, Seppälä A, Saari K, Seitsonen J, Ruokolainen J, Puiisto S, et al. Influence of particle size and shape on turbulent heat transfer characteristics and pressure losses in water-based nanofluids. *Int J Heat Mass Transf*. 2013;61:439–48.
15. Ranga Babu JA, Kumar KK, Srinivasa RS. State-of-art review on hybrid nanofluids. *Renew Sustain Energy Rev*. 2017;77:551–65.
16. Yarmand H, Gharehkhani S, Ahmadi G, Shirazi SFS, Baradaran S, Montazer E, et al. Graphene nanoplatelets-silver hybrid nanofluids for enhanced heat transfer. *Energy Convers Manag*. 2015;100:419–28. <https://doi.org/10.1016/j.enconman.2015.05.023>.
17. Baby TT, Sundara R. Synthesis and transport properties of metal oxide decorated graphene dispersed nanofluids. *J Phys Chem C*. 2011;115:8527–33. <https://doi.org/10.1021/jp200273g>.
18. Munkhbayar B, Tanshen MR, Jeoun J, Chung H, Jeong H. Surfactant-free dispersion of silver nanoparticles into MWCNT-aqueous nanofluids prepared by one-step technique and their thermal characteristics. *Ceram Int*. 2013;39:6415–25. <https://doi.org/10.1016/j.ceramint.2013.01.069>.
19. Tadjarodi A, Zabihi F. Thermal conductivity studies of novel nanofluids based on metallic silver decorated mesoporous silica nanoparticles. *Mater Res Bull*. 2013;48:4150–6. <https://doi.org/10.1016/j.materresbull.2013.06.043>.
20. Suresh S, Venkitaraj KP, Selvakumar P, Chandrasekar M. Synthesis of  $\text{Al}_2\text{O}_3$ -Cu/water hybrid nanofluids using two-step method and its thermophysical properties. *Colloids Surf A Physicochem Eng Asp*. 2011;388:41–8. <https://doi.org/10.1016/j.colsurfa.2011.08.005>.
21. Esfe MH, Yan W, Akbari M, Karimipour A, Hassani M. Experimental study on thermal conductivity of DWCNT-ZnO/water-EG nanofluids. *Int Commun Heat Mass Transf*. 2015. <https://doi.org/10.1016/j.icheatmasstransfer.2015.09.001>.
22. Madhesh D, Parameshwaran R, Kalaiselvam S. Experimental investigation on convective heat transfer and rheological characteristics of Cu-TiO<sub>2</sub> hybrid nanofluids. *Exp Therm Fluid Sci*. 2014;52:104–15. <https://doi.org/10.1016/j.expthermflusci.2013.08.026>.
23. Yarmand H, Gharehkhani S, Shirazi SFS, Goodarzi M, Amiri A, Sarsam WS, et al. Study of synthesis, stability and thermo-physical properties of graphene nanoplatelet/platinum hybrid nanofluid. *Int Commun Heat Mass Transf*. 2016;77:15–21. <https://doi.org/10.1016/j.icheatmasstransfer.2016.07.010>.
24. Yarmand H, Gharehkhani S, Shirazi SFS, Amiri A, Montazer E, Arzani HK, et al. Nanofluid based on activated hybrid of biomass carbon/graphene oxide: Synthesis, thermo-physical and electrical properties. *Int Commun Heat Mass Transf*. 2016;72:10–5. <https://doi.org/10.1016/j.icheatmasstransfer.2016.01.004>.
25. Sundar LS, Singh MK, Sousa ACM. Enhanced heat transfer and friction factor of MWCNT-Fe<sub>3</sub>O<sub>4</sub>/water hybrid nanofluids. *Int Commun Heat Mass Transf*. 2014;52:73–83. <https://doi.org/10.1016/j.icheatmasstransfer.2014.01.012>.

26. Hemmat Esfe M, Abbasian Arani AA, Rezaie M, Yan WM, Karimipour A. Experimental determination of thermal conductivity and dynamic viscosity of Ag-MgO/water hybrid nanofluid. *Int Commun Heat Mass Transf.* 2015;66:189–95. <https://doi.org/10.1016/j.icheatmasstransfer.2015.06.003>.
27. Goodarzi M, Toghraie D, Reiszadeh M, Afrand M. Experimental evaluation of dynamic viscosity of ZnO–MWCNTs/engine oil hybrid nanolubricant based on changes in temperature and concentration. *J Therm Anal Calorim.* 2018. <https://doi.org/10.1007/s10973-018-7707-8>.
28. Toghraie D, Chaharsoghi VA, Afrand M. Measurement of thermal conductivity of ZnO–TiO<sub>2</sub>/EG hybrid nanofluid. *J Therm Anal Calorim.* 2016;125:527–35. <https://doi.org/10.1007/s10973-016-5436-4>.
29. Zadkhast M, Toghraie D, Karimipour A. Developing a new correlation to estimate the thermal conductivity of MWCNT–CuO/water hybrid nanofluid via an experimental investigation. *J Therm Anal Calorim.* 2017;129:859–67.
30. Esfe MH, Behbahani PM, Akbar A, Arani A, Sarlak MR. Thermal conductivity enhancement of SiO<sub>2</sub>–MWCNT (85:15%)—EG hybrid nanofluids. *J Therm Anal Calorim.* 2017;128:249–58.
31. Esfe MH, Amiri MK, Alirezaie A. Thermal conductivity of a hybrid nanofluid A new economic strategy and model. *J Therm Anal Calorim.* 2018. <https://doi.org/10.1007/s10973-017-6836-9>.
32. Devendiran DK, Amirtham VA. A review on preparation, characterization, properties and applications of nanofluids. *Renew Sustain Energy Rev.* 2016;60:21–40. <https://doi.org/10.1016/j.rser.2016.01.055>.
33. Chougule SS, Sahu SK. Enhancement of heat transfer with nanofluids. IIT Indore; 2015. <http://hdl.handle.net/123456789/51>. Accessed 24 June 2018.
34. Freitas C, Müller RH. Effect of light and temperature on zeta potential and physical stability in solid lipid nanoparticle (SLN<sup>®</sup>) dispersions. *Int J Pharm.* 1998;168:221–9.
35. Keblinski P, Phillpot SR, Choi SUS, Eastman JA. Mechanisms of heat flow in suspensions of nanosized particles (nanofluids). *Int J Heat Mass Transf.* 2002;45:855–63.